Research Article

Developing and Implementing a Quantum Algorithm for the Sliding Mode Controller Using Multiple Qubit Operators: Application to DC Motor Speed Drive

Nadjet Zioui*
Department of Mechanical Engineering, Université du Québec à Trois-Rivières, Quebec, Canada

Aicha Mahmoudi
Université de Sherbrooke, Quebec, Canada

Mohamed Tadjine
LCP (Laboratoire de Commande des Processus), École Nationale Polytechnique d'Alger, El Harrach, Algiers

* Corresponding author. E-mail: nadjet.zioui@uqtr.ca

Abstract

With the advent of quantum computing, almost all classical computing concepts must be translated into quantum equivalents. Control theory, in particular, requires a large numbers of calculations. This paper designs and presents a quantum sliding mode controller. The controller uses two qubit states, one for detecting tracking errors and the other for determining the signs of the errors. The control signal to be applied to the system is stored in the third qubit state. This new controller is implemented on a DC motor to control the angular velocity using electrical current as an input signal. In terms of tracking error energy performance, the results show that the quantum sliding mode controller is just as efficient as the classical sliding mode controller. However, the quantum controller outperforms its predecessor by using 76% to 79% less control energy, allowing for smaller actuators. This represents a significant advancement in control theory in the era of quantum computers. Indeed, actuator control energy is the main drawback of the classical sliding mode control and reducing this energy is one of the main challenges for the control community.

Keywords: Actuator control effort, Hadamard and Toffoli gates, Quantum computing, Quantum robust controller, Qubit states, Sliding mode

1 Introduction

Quantum computing is a new paradigm that has captured the scientific community's attention in recent decades. Many countries have invested significantly in quantum computing strategies due to the enormous potential of exponentially accelerating computation, as well as the promising information security applications. Especially in engineering, there has been extensive research into using quantum computing tools to solve problems and developing new quantum computing packages. Specifically in automatic control, some efforts have been made to adapt the control theory to the new quantum reality. State domain equations have been adapted to quantum computing using qubit states, and a solution-based HHL algorithm, a quantum algorithm named after its three creators (Harrow, Hassidim, and Lloyd), that solves a system of linear equations, was presented and compared to the exact classical solution in [1]. In the quantum state domain, a backstepping controller-based linearising decoupling controller has also been investigated, and a new quantum controller has been introduced [2].

The sliding mode controller, on the other hand, is a well-known and widely used robust control strategy. It is based on the choice of a sliding manifold

on which control objectives are met [3]–[6]. The controller draws the state vector to the sliding manifold and keeps it there indefinitely [7]–[10]. Few studies have addressed the sliding mode control technique in the context of quantum computing. Several works have been reported with a focus on using the classical sliding mode controller to control quantum systems [11]–[15]. Other works have used sliding mode control to achieve quantum state control [16]–[18]. Others have attempted to improve the classical sliding mode controller using existing quantum computing tools, for example, by employing an adaptive quantum neural network to improve the speed of the sliding mode controller for the position of an induction motor [19]. A quantum genetic algorithm was used to improve the chattering and robustness to the noise of a sliding mode controller [20]. A quantum particle swarm optimisation in conjunction with a sliding mode controller has also been considered for vibration suppression in a multilayer composite material plate system [21]. Furthermore, researchers have proposed using sliding mode in conjunction with quantum logic to control a helicopter [22]. The authors state that they used quantum logic to improve control accuracy. However, the presented methodology lacks details on how to use quantum computing to achieve the stated goals. Furthermore, no sliding mode control strategies based on quantum states aimed at time-varying tracking problems have been identified in the preceding works.

Other works in the literature have attempted to define a quantum sliding mode control by choosing the sliding manifold as a qubit state, such as [23], whose authors defined a sliding surface as a formula that takes into account the measurement of the difference between two qubit states. Without providing any proof, the authors assumed that the control objectives were met on their sliding surfaces. Furthermore, the authors assumed that the system's initial configuration is on the sliding surface, which is not always the case in practice. None of the works found in the literature takes into account time-varying time for tracking purposes, nor did they present concrete implementations for real engineering systems, nor did they present quantum circuits for validation.

To the best of the authors' knowledge, no published works have presented the quantum sliding mode control strategy for tracking problems, along with quantum circuit implementation and validation on a real dynamical system. In fact, with the introduction of quantum computers, nearly everything in the traditional computing world must be adapted to the new quantum computing reality. From this perspective, this paper proposes a quantum sliding mode control strategy for the first time, taking into account two control qubit states representing the tracking error and its sign, as well as a target qubit state describing the control signal to be applied to the system. The simulation results on a direct current (DC) motor speed control show that the new controller outperforms its predecessor by using 76% to 79% less control effort, allowing for smaller actuators. This opens the door for the design of a robust sliding mode controller using reduced energy actuators.

2   Qubits and Quantum Operators

The qubit is the fundamental unit of information in quantum computing, with infinitely many possible states that are combinations of two eigenstates 0 (denoted as $|0\rangle$) and 1 (denoted as $|1\rangle$) [24]–[27]. A qubit state $|q\rangle$ can be written as Equation (1)

$$|q\rangle = \alpha|0\rangle + \beta|1\rangle \tag{1}$$

where α and β are complex numbers that can be seen as the projections of $|q\rangle$ onto the two basis states $|0\rangle$ and $|1\rangle$, respectively, such that $\sqrt{|\alpha|^2 + |\beta|^2} = 1$.

Quantum operators can change the states of qubits. The Identity, X, Y, and Z gates are the fundamental quantum operators that each manipulate only one qubit state. Their matrix representations are as shown in Equation (2):
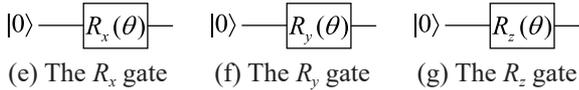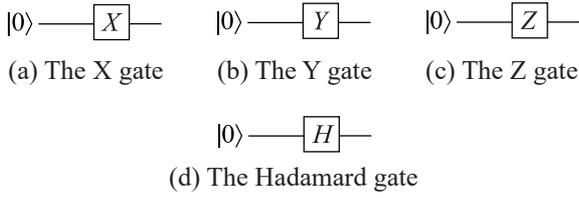
$$\boldsymbol{I} = \begin{pmatrix} 1 & 0 \\ 0 & 1 \end{pmatrix} \tag{2.1}$$

$$\boldsymbol{X} = \begin{pmatrix} 0 & 1 \\ 1 & 0 \end{pmatrix} \tag{2.2}$$

$$\boldsymbol{Y} = \begin{pmatrix} 0 & -i \\ i & 0 \end{pmatrix} \tag{2.3}$$

$$\boldsymbol{Z} = \begin{pmatrix} 1 & 0 \\ 0 & -1 \end{pmatrix} \tag{2.4}$$

There are also other operators, such as the Hadamard gate H and the three basic rotation gates, which are defined in Equations (3) and (4), respectively:

(a) The X gate   (b) The Y gate   (c) The Z gate

(d) The Hadamard gate

(e) The R_x gate   (f) The R_y gate   (g) The R_z gate

Figure 1: The quantum circuit representations of the basic one-qubit operators.

$$H = \begin{pmatrix} 1/\sqrt{2} & 1/\sqrt{2} \\ 1/\sqrt{2} & -1/\sqrt{2} \end{pmatrix} \tag{3}$$

$$R_x(\theta) = \begin{pmatrix} \cos\theta & i\sin\theta \\ i\sin\theta & \cos\theta \end{pmatrix} \tag{4.1}$$

$$R_y(\theta) = \begin{pmatrix} \cos\theta & \sin\theta \\ -\sin\theta & \cos\theta \end{pmatrix} \tag{4.2}$$

$$R_z(\theta) = \begin{pmatrix} \cos\theta & i\sin\theta \\ i\sin\theta & -\cos\theta \end{pmatrix} \tag{4.3}$$
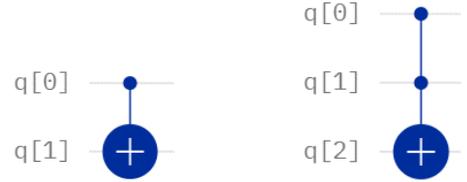
Quantum circuits can be used to implement quantum operators. The quantum circuits are typically represented by horizontal lines for the qubit states and boxes for the operators, as shown in Figure 1 for the one-qubit operators presented above.

There are also operators in quantum computing that act on two or more qubits. In the following, two particular gates are presented, namely the controlled NOT (CNOT) gate and the Toffoli or controlled CNOT (CCNOT) gate [26].

The CNOT gate makes use of two qubits. It modifies the target qubit $|q_0\rangle$ if and only if the control qubit $|q_1\rangle$ is in the state $|1\rangle$. The operation of this gate is summarised in Table 1.

Table 1: The CNOT gate truth table

Before Operation		After Operation	
$|q_0\rangle$	$|q_1\rangle$	$|q_0\rangle$	$|q_1\rangle$
$|0\rangle$	$|0\rangle$	$|0\rangle$	$|0\rangle$
$|1\rangle$	$|0\rangle$	$|1\rangle$	$|0\rangle$
$|0\rangle$	$|1\rangle$	$|1\rangle$	$|1\rangle$
$|1\rangle$	$|1\rangle$	$|0\rangle$	$|1\rangle$

(a) The CNOT gate   (b) The CCNOT gate

Figure 2: The CNOT and CCNOT quantum circuits using IBM Quantum Composer [28].

The Toffoli gate requires two control qubits $|q_1\rangle$ and $|q_2\rangle$. Only if both control qubits are in the state $|1\rangle$ is the target qubit change. The operation of this gate is summarised in Table 2, and Figure 2 depicts the quantum circuits used to implement the CNOT and CCNOT operators.

Table 2: The CCNOT gate truth table

Before Operation			After Operation		
$|q_0\rangle$	$|q_1\rangle$	$|q_2\rangle$	$|q_0\rangle$	$|q_1\rangle$	$|q_2\rangle$
$|0\rangle$	$|0\rangle$	$|0\rangle$	$|0\rangle$	$|0\rangle$	$|0\rangle$
$|1\rangle$	$|0\rangle$	$|0\rangle$	$|1\rangle$	$|0\rangle$	$|0\rangle$
$|0\rangle$	$|1\rangle$	$|0\rangle$	$|0\rangle$	$|1\rangle$	$|0\rangle$
$|1\rangle$	$|1\rangle$	$|0\rangle$	$|1\rangle$	$|1\rangle$	$|0\rangle$
$|0\rangle$	$|0\rangle$	$|1\rangle$	$|0\rangle$	$|0\rangle$	$|1\rangle$
$|1\rangle$	$|0\rangle$	$|1\rangle$	$|1\rangle$	$|0\rangle$	$|1\rangle$
$|0\rangle$	$|1\rangle$	$|1\rangle$	$|1\rangle$	$|1\rangle$	$|1\rangle$
$|1\rangle$	$|1\rangle$	$|1\rangle$	$|0\rangle$	$|1\rangle$	$|1\rangle$

The required linear algebraic concepts are the inner and outer products. The inner product is used to calculate the overlap between two quantum states. The inner product of two qubits $|q_1\rangle = \alpha_1 |0\rangle + \beta_1 |1\rangle$ and $|q_2\rangle = \alpha_2 |0\rangle + \beta_2 |1\rangle$ is denoted as $\langle q_1 | q_2 \rangle$ and is defined as in Equation (5) [25]:

$$\langle q_1 | q_2 \rangle = \alpha_2^\dagger \alpha_1 + \beta_2^\dagger \beta_1 \tag{5}$$

where $c^\dagger$ denotes the complex conjugate of c.

A matrix is produced by the outer product of two states. The outer product of the two states $|q_1\rangle = \alpha_1 |0\rangle + \beta_1 |1\rangle$ and $|q_2\rangle = \alpha_2 |0\rangle + \beta_2 |1\rangle$ is denoted by $|q_1\rangle\langle q_2|$ and is defined as in Equation (6):

$$|q_1\rangle\langle q_2| = \begin{pmatrix} \alpha_1 \\ \beta_1 \end{pmatrix} \begin{pmatrix} \alpha_2^\dagger & \beta_2^\dagger \end{pmatrix} = \begin{pmatrix} \alpha_1\alpha_2^\dagger & \alpha_1\beta_2^\dagger \\ \beta_1\alpha_2^\dagger & \beta_1\beta_2^\dagger \end{pmatrix} \tag{6}$$

The goal of measurement is to convert quantum

information (stored in the quantum system) into classical information. Measuring a qubit is analogous to reading a classical bit to determine whether its state is 0 or 1. The fact that measurement outcomes are probabilistic is a fundamental principle of quantum mechanics.

The inner product notation is used for measurement. For the case of a single-qubit state, the probability that the qubit $|q\rangle$ is at state $|0\rangle$ after the measurement is $\langle 0|q\rangle|^2$, and the probability of it being at state $|1\rangle$ is $\langle 1|q\rangle|^2$. As a result, measurement probabilities can be represented as the absolute values of overlaps squared.

The measurement concept can be generalised to multiple-qubit cases or systems of qubits. After measuring n qubit states $|\phi\rangle$, the probability of obtaining the bit string $|x_1 ...x_n$ is then $|\langle x_1 ...x_n |\phi\rangle|^2$ [26]. For example, in a three-qubit state $|\phi\rangle=|q_0 q_1 q_2\rangle$, if the goal is to determine whether the qubit state $|q_0\rangle$ is $|0\rangle$, the probability is calculated as in Equation (7):

$$P\left(|q_0 = |0\rangle\right) = \sum_{\{q_1,q_2\}\in\{0,1\}}|\langle 0q_1q_2 |\phi\rangle|^2 \tag{7}$$

3 State Domain Equations and Sliding Mode Control

State domain equations are a powerful tool for modelling dynamical systems in the field of control engineering. They are used extensively to help formulate specific problems by describing the relationships between unknown physical signals and variables. Linear systems are widely used in automation and control to describe the dynamics of a variable given an input signal. The system's desired behavior is then controlled using state feedback or linear quadratic controllers, for example.

In the state domain, a set of n first-order equations is used to represent the system, where n is the overall system order. The equations for a nonlinear system are as follows Equation (8):

$$\begin{cases} \dot{x} = f\left(x\right)+g\left(x\right)u \\ y = h\left(x\right) \end{cases} \tag{8}$$

where $x \in \mathbb{R}^n$ is the state domain vector, $\dot{x}$ is the first-order time derivative of x, $y \in \mathbb{R}^p$ is the output vector, $u \in \mathbb{R}^m$ is the control vector, and $f(x) \in \mathbb{R}^n$, $g(x) \in \mathbb{R}^{n\times m}$, and $h(x) \in \mathbb{R}^p$ are vector distributions.

For a linear system, this becomes [Equation (9)]

$$\begin{cases} \dot{x} = Ax + Bu \\ y = Cx \end{cases} \tag{9}$$

where $A \in \mathbb{R}^{n \times n}$, $B \in \mathbb{R}^{n\times m}$, and $C \in \mathbb{R}^{p\times n}$ are the state, control, and output matrices. In particular, for a first-order system, this can be written as follows:

$$\begin{cases} \dot{x} = ax + bu \\ y = cx \end{cases} \tag{10}$$

where a, b, and c are real numbers.

The state vector contains the system variables, including the system output signals, whereas the control vector contains the system input variables that must be adjusted to achieve a specific behavior for the system output.

Assuming that the system is controllable, the control problem is to compute the control variable u to obtain a specific behavior for the state vector, using a variety of strategies that are primarily determined by the structure of the state equations on the one hand and the control objectives on the other. For most applications, the output of the system is the state variable itself. Otherwise, it is always possible to adjust the reference signal accordingly.

For tracking purposes, the interest is focused on the tracking error $e = x - x_r$ rather than on the state vector itself. The reference for the state variable x is x_r. As a result, system Equation (10) can be written as follows:

$$\dot{e} = ax + bu - \dot{x}_r \tag{11}$$

A linearising decoupling controller is typically used for nonlinear systems (as well as linear systems), resulting in n first-order subsystems that can be controlled independently. As a result, the following discussion will solely consider first-order systems. When applied to system Equation (11), the linearising decoupling controller Equation (12) produces system Equation (13).

$$u = b^{-1}\left(-ax + \dot{x}_r + v\right) \tag{12}$$
$$\dot{e} = v \tag{13}$$

where v is the new virtual control signal.

The control problem for systems Equation (13) is then to compute the new virtual control variable *v* to obtain a specific behavior for the tracking error, specifically to nullify it, using several control strategies. One of the robust control strategies that can be used in this case is the sliding mode control.

The sliding mode is a well-known and widely used robust controller. It relies on the definition of a sliding surface $S(e)$ at which the control objectives are achieved. This means that when $S = 0$, the tracking error is asymptotically stable at zero, and therefore the state variable has reached its reference. The sliding mode control is achieved by following two fundamental conditions, which are:

1) Attractiveness, $S\dot{S} \leq 0$, which can be interpreted as the need for the system to converge towards its control objective. This is achieved by imposing $\dot{S} = -K\,\text{sign}(S)$, where K is a positive constant. This leads to finite-time convergence of S to zero.

2) Invariance, $\dot{S} = 0 \Rightarrow S = 0$, that is, once the control objective is met, there is no need to move the system away from it [Equation (14)].

$$\dot{S}(e) = \frac{\partial S}{\partial e} \times \frac{\partial e}{\partial t} = \frac{\partial S}{\partial e}\dot{e} = \frac{\partial S}{\partial e}(v) \tag{14}$$

Highlighting the relationship with the state domain Equation (10). Both the attractiveness and invariance conditions are met by the expression Equation (12) for the control variable *v*. In fact, it will produce $\dot{S} = -K\,\text{sign}(S)$, where K is a positive constant. If the sliding surface is chosen to be the tracking error $S = e$, then $\frac{\partial S}{\partial e} = 1$, further simplifying the controller's computation to Equation (15).

$$v = -K\left(\frac{\partial S}{\partial e}\right)^{-1}\text{sign}(S) \tag{15}$$

4 Methods

The definition of each qubit state used as part of the solution must be established to implement the quantum sliding mode controller. If there is a nonzero tracking error, the sliding mode controller will apply a negative control value -K if the error is positive and a positive control value K if the error is negative. However, if there is no error, then the control signal is zero as well. As a result, the action is controlled by two parameters:

1) the presence of an error and 2) the sign of the error. The two parameters are expressed as two qubit states: $|q_1\rangle$ for the presence of the error and $|q_2\rangle$ for its sign. Tables 3 and 4 show how these two qubits work and what each of their states means.

Table 3: The logic of operation of the qubit state $|q_1\rangle$

State	Meaning
$|0\rangle$	The error is zero
$|1\rangle$	The error is nonzero

Table 4: The logic of operation of the qubit state $|q_2\rangle$

State	Meaning
$|0\rangle$	The error is negative
$|1\rangle$	The error is positive

The sliding mode controller implementation will use these two qubits, along with a third qubit state $|v\rangle$ (or $|q_0\rangle$), to decide the control that will be applied to the system. Table 5 summarises the logic that describes this operation.

**Table 5**: The truth table of the quantum sliding mode control

Initial states			Final states		
$|v\rangle$	$|q_1\rangle$	$|q_2\rangle$	$|v\rangle$	$|q_1\rangle$	$|q_2\rangle$
$|v\rangle$	$|0\rangle$	$|q_2\rangle$	$|0\rangle$	$|0\rangle$	$|q_2\rangle$
$|v\rangle$	$|1\rangle$	$|0\rangle$	$-|1\rangle$	$|1\rangle$	$|0\rangle$
$|v\rangle$	$|1\rangle$	$|1\rangle$	$|1\rangle$	$|1\rangle$	$|1\rangle$

A quantum circuit involving Hadamard and CCNOT gates is proposed to implement the operation in Table 5. The Hadamard gate is used for two reasons: 1) to introduce a balanced distribution of coefficients, and 2) to introduce a negative sign, which is required for the control strategy. The proposed algorithm, with the corresponding quantum circuit shown in Figure 3, is therefore [Equation (16)].

$$|\varphi\rangle = \text{CCNOT}(u, q_1, Hq_2) \tag{16}$$

where $|\varphi\rangle$ is the system of qubits $|v, q_1, q_2\rangle$.

The control signal is then obtained by applying the inner product to the bit string $|101\rangle$, the same way as the measurement is performed except that the norm is not computed to avoid the loss of the signal sign of the control variable, which is essential for the control strategy.
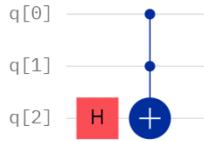
Figure 3: The quantum circuit of the quantum sliding mode controller (image generated using IBM Quantum Composer [28]).
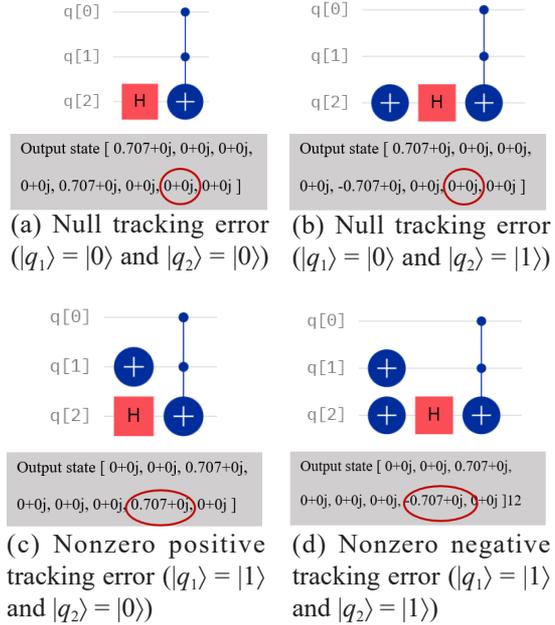
5   Results and Discussion

The proposed solution was implemented using the IBM Quantum Composer online simulator and Matlab (R2021a) for real-time reference tracking simulation.

To validate the open-loop controller operation, the quantum circuit in Figure 3 has been implemented and tested in three different configurations: 1) null tracking error (taking into account both possible states $|0\rangle$ and $|1\rangle$ for the qubit state $|q_1\rangle$), 2) nonzero positive tracking error, and 3) nonzero negative tracking error. Figure 4 depicts the execution of the three tests as well as their results.

Figure 4 shows that the proposed circuit performs the sliding mode control. An appropriate amplification is then required to compensate for the value $\sqrt{2}/2$ introduced by the Hadamard gate and to tune the desired dynamics with the gain K. To validate the closed-loop operation, the proposed solution was implemented using Matlab code to create a simulator for the controlled system's state equations. The functional diagram of the control system is shown in Figure 5.

For the simulation, the system Equation (10) has been implemented with the parameters taking the values $a = -0.1$ and $b = 0.1$. This is a typical state domain model for a DC motor considering the current I

(a) Null tracking error ($|q_1\rangle = |0\rangle$ and $|q_2\rangle = |0\rangle$)

(b) Null tracking error ($|q_1\rangle = |0\rangle$ and $|q_2\rangle = |1\rangle$)

(c) Nonzero positive tracking error ($|q_1\rangle = |1\rangle$ and $|q_2\rangle = |0\rangle$)

(d) Nonzero negative tracking error ($|q_1\rangle = |1\rangle$ and $|q_2\rangle = |1\rangle$)

Figure 4: Validation of the operation of the quantum sliding controller using the online quantum simulator IBM Quantum Composer [28].

as the control signal and the angular velocity ω as an output signal, which is also the state variable of the system. In fact, the dynamical equation of a DC motor is represented by Equation (17).

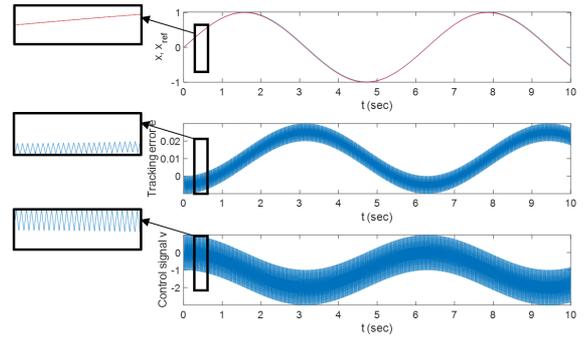$$J \, d\omega/dt = K_a I - B_m \omega \tag{17}$$

With the parameters of the DC motor summarised in Table 6, this can be rewritten in the form of the state Equation (10) by dividing the whole equation by J, which leads to the selected values for the parameters a and b.
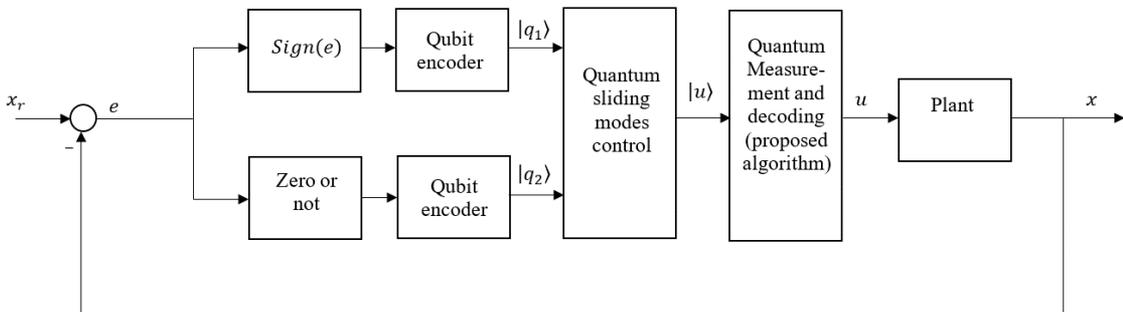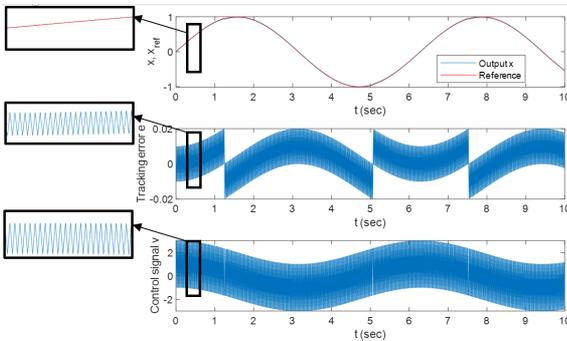

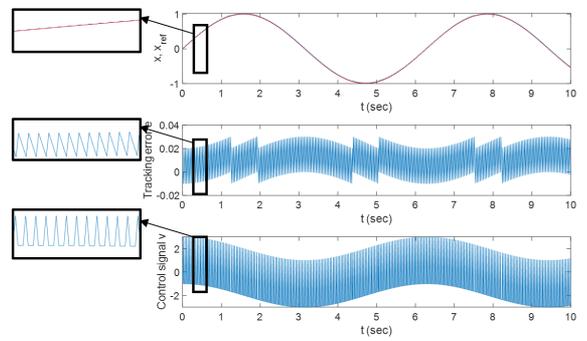
Figure 5: Diagram of the quantum sliding mode control.
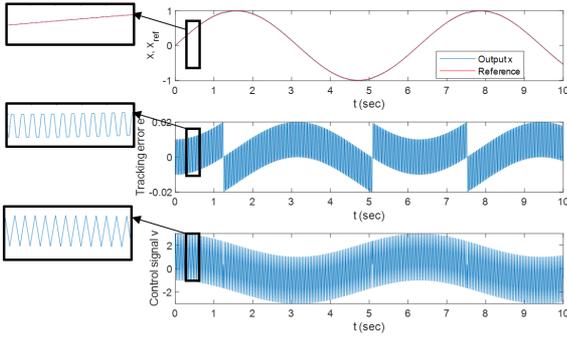
Figure 6: Simulation results for the quantum sliding mode control.

Figure 7: Simulation results for the classical sliding mode control.

Figure 8: Simulation results for the quantum sliding mode control in the presence of a disturbance.

Figure 9: Simulation results for the classic sliding mode control in the presence of a disturbance.

Table 6: The parameters of the DC motor

| Parameter	Description	Value (Unit)
J	Inertia constant	1 kg .m^2
K_a	Current constant	0.1 N .m/A
B_m	Viscous friction constant	0.1 N .m .s

Figures 6 and 7 illustrate the simulation results for the quantum and classical sliding mode controllers, respectively. The insets show enlarged regions around 500 ms to better compare the signal waves for both control strategies.

From the above results, it appears that both classical and quantum sliding mode strategies achieved good dynamical reference tracking objectives. However, it can be seen that the quantum sliding mode controller presented a less energetic control signal compared to its counterpart, which used 76.3% more energy, with $\sum v^2 = 2522$ for the former and $\sum v^2 = 4522$ for the latter. Both strategies showed the same energy of the error with $\sum e^2 = 0.1385$ for both methods.

A constant disturbance of 1% on the reference has been introduced in both models to evaluate the robustness of the two controllers in the presence of disturbances. For a reference speed of 1500 rpm, this would represent a 15 rpm error on the speed of the motor. Figures 8 and 9 illustrate the results for this case.

The above simulation results highlight that both the classical and quantum sliding mode controllers achieved robustness in the presence of a constant disturbance. However, the classical sliding mode controller consumed more energy with $\sum v^2 = 4628.4$, 76.11% more than its counterpart, which recorded $\sum v^2 = 2628.1$, as illustrated in Figure 10. The same trend was observed for the energy of the error for both sliding mode controllers, which were both about $\sum e^2 = 0.25$, as depicted in Figure 11.

It can be said that both sliding mode controllers have equivalent performances with regard to the tracking error and the energy of error. However, the quantum controller outperformed its classic counterpart in
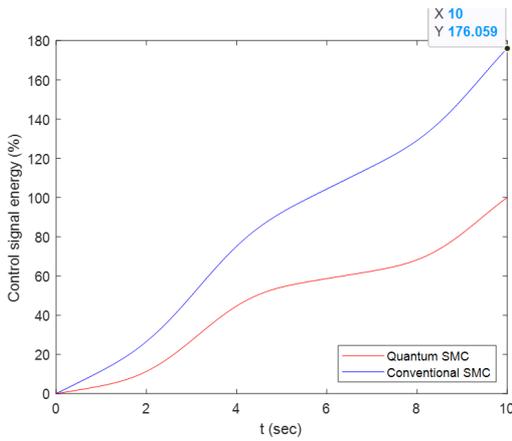
Figure 10: Evolution of control signal energy in % over time.
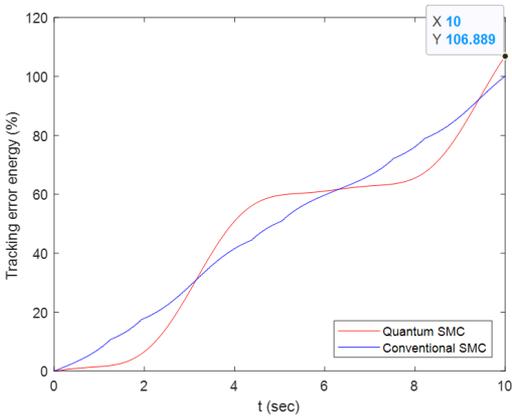
Figure 11: Evolution of tracking error energy in % over time.

Figure 12: Simulation results for the classical sliding mode control.

Figure 13: Simulation results for the proposed quantum sliding mode control.
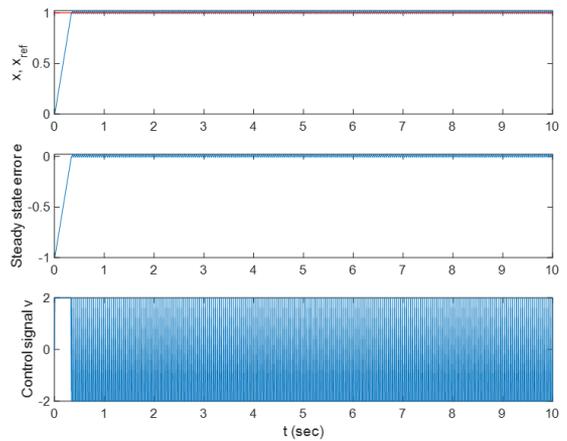
terms of control energy with or without the presence of disturbances.
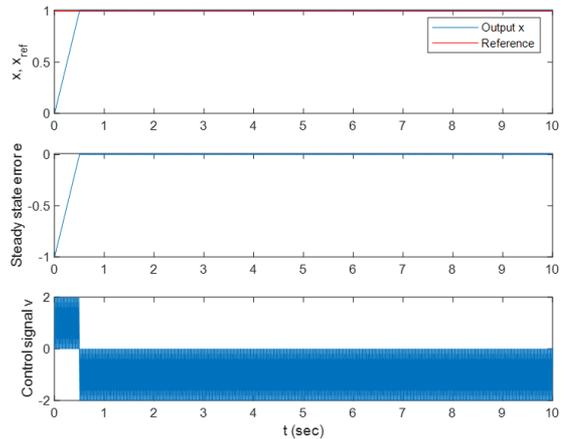
5 Further Analysis

To compare the performance of the proposed controller with the works in the literature, a constant reference is considered in the following, and a comparative analysis is provided with regard to the steady error and the settling time, both for the classical and the proposed quantum controller.

Figures 12 and 13 depict the speed results for the classical and quantum control strategies, respectively.

The above simulation results highlight that both controllers achieved good stabilisation performance

with a constant reference in the presence of a constant disturbance. However, the classical sliding mode controller consumed more energy with $\sum v^2 = 4000$, which is 100% more than its counterpart, which recorded $\sum v^2 = 2000$.

With respect to steady-state error, both the classical and quantum sliding mode controllers offer similar properties. However, in terms of control energy, the quantum controller surpassed its classical equivalent.

Table 7 summarises a comparative analysis of the results of the sliding mode controllers for DC motors that have been found in the literature along with the classical sliding mode developed in this paper and the proposed quantum version. The values have
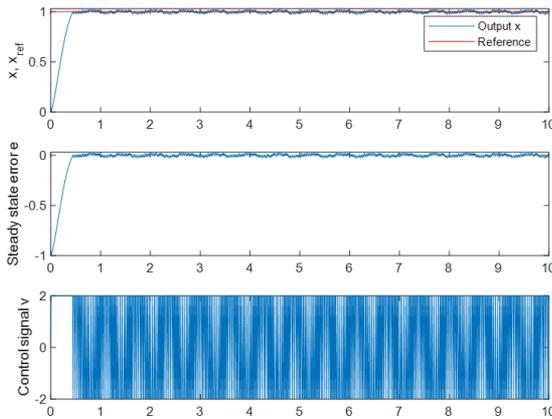
Figure 14: Simulation results for the classical sliding mode control with dynamic disturbance.

Figure 15: Simulation results for the proposed quantum sliding mode control with dynamic disturbance.

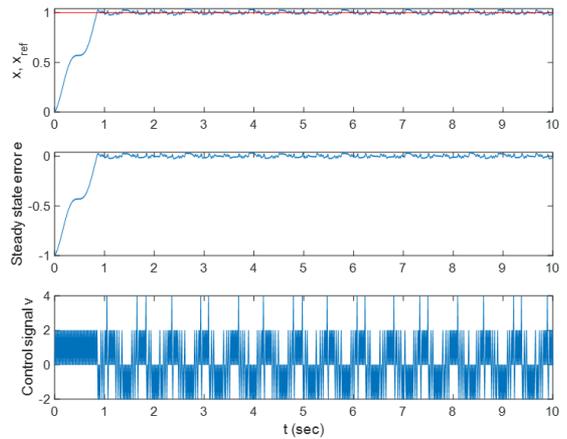been normalised to allow a better comparison as the dynamics of the DC motors are different.

Table 7: A comparative analysis of performance with works in the literature

Reference	Settling Time (s)	Steady-state Error
Maheswararao *et al.* [3]	0.067	−0.02
Dursun *et al.* [5]	0.023	0
Ramprasad *et al.* [7]	0.643	0
Bharathi *et al.* [8]	0.031	0
Our classical sliding mode controller	0.035	0.005
The proposed quantum sliding mode controller	0.05	0.005

Table 7 shows that the settling times for both the classical and quantum sliding mode controllers are within the range of data available in the literature, with the classical controller having a slightly better value. The steady-state error, on the other hand, is close to zero for both controllers.

Another relevant case study was the examination of the behavior of controlled motors in the presence of a dynamic disturbance. A 1% amplitude sine wave with a frequency of $10/2\pi$ Hz was introduced. Figures 14 and 15 show the outcome of this case study.

The simulation findings show that both controllers performed well in terms of stabilisation with a constant reference in the presence of a dynamic disturbance. The original sliding mode controller, on the other hand,

consumed 77.6% more energy, with $\sum v^2 = 2252$, than its counterpart, for which $\sum v^2 = 4000$.

In terms of steady-state error, both the classical and quantum sliding mode controllers offer comparable characteristics. However, in terms of control energy, the quantum controller surpassed its classical equivalent.

4 Conclusions

This paper presented the formalism of a quantum sliding mode control using two qubit states as an error detector and error sign indicator to provide a target qubit state used as a control variable. Unlike the works found in the literature, we have presented a detailed operating principle and provided an implementation using a quantum circuit with an application to a real system, namely the DC motor speed control. The results show that the proposed controller outperforms the standard sliding mode controller while using significantly less control energy to achieve the same tracking error performance. A comparative examination of the related works available in the literature was also undertaken for stabilisation problems. This revealed that our controllers show typical settling times and acceptable steady-state errors. The findings of this work should contribute significantly to the reduction of actuator control effort, by showing that smaller actuators can be employed using the quantum sliding modes controller, providing the same error performance as larger actuators under the classical sliding modes controller. This may be useful in a variety of engineering

applications, such as electric vehicles.

Acknowledgements

Author Contributions

N.Z.: conceptualisation, investigation, methodology, research design, data analysis, writing an original draft, reviewing and editing, project administration; A.M.: investigation, methodology, research design, data analysis, writing an original draft; M.T.: research design, data analysis, data curation, writing—reviewing and editing, project administration. All authors have read and agreed to the published version of the manuscript.

Conflicts of Interest

The authors declare no conflict of interest.

References

[1] M. E. A. Boudjoghra, S. A. F. Daimellah, N. Zioui, Y. Mahmoudi, and M. Tadjine, "State-domain equations and their quantum computing solution based HHL algorithm," *Mathematical Modelling of Engineering Problems*, vol. 9, pp. 879–886, Aug. 2022, doi: 10.18280/mmep.090404.

[2] N. Zioui, A. Mahmoudi, and M. Tadjine, "Design of a new hybrid linearizing-backstepping controller using quantum state equations and quantum spins," *International Journal of Automation and Control*, vol. 17, pp. 397–417, Apr. 2023, doi: 10.1504/IJAAC.2023.10051373.

[3] U. Maheswararao Ch, Y. S. Kishore Babu, and K. Amaresh, "Sliding mode speed control of a DC motor," in *2011 International Conference on Communication Systems and Network Technologies*, pp. 387–391 Jun. 2011, doi: 10.1109/CSNT.2011.86.

[4] P. Ghalimath and S. S. Sankeswari, "Speed control of DC motor using sliding mode control approach," *IOSR Journal of Electrical and Electronics Engineering*, vol. 10, pp. 17–22,

Jul. 2015, doi: 10.9790/1676-10411722.

[5] E. H. Dursun and A. Durdu, "Speed control of a DC motor with variable load using sliding mode control," *International Journal of Computer and Electrical Engineering*, vol. 8, pp. 219–226, Jun. 2016, doi: 10.17706/ijcee.2016.8.3.219-226.

[6] S. Vaez-Zadeh and M. Zamanian, "Permanent magnet DC motor sliding mode control system," *IJE Transactions A: Basics*, vol. 16, pp. 367–376, Nov. 2003.

[7] B. Ramprasad and K. Venkataratnam, "A novel speed control of DC motor using sliding mode technique," *International Journal of Current Engineering and Scientific Research*, vol. 6, pp. 40–46, 2019.

[8] N. Bharathi, A. Kavitha, and B. Barathy, "Sliding mode control for speed control of brushless DC motor," *International Journal of Scientific and Engineering Research*, vol. 5, pp. 22–27, Apr. 2014.

[9] F. D. Chizea, E. Ovie, C. M. Akachukwu, and M. B. Muazu, "Sliding mode control of a miniature brushless DC motor," *International Journal of Engineering and Technical Research*, vol. 9, pp. 24–27, Aug. 2019.

[10] H. Guldemir, "Sliding mode speed control for DC drive systems," *Mathematical and Computational Applications*, vol. 8, pp. 377–384, 2003.

[11] B. R. Jo, H. W. Ahn, and M. J. Youn, "Multi-variable sliding mode control of quantum boost SRC," *IEEE Transactions on Control Systems Technology*, vol. 2, pp. 148–150, Jun. 1994, doi: 10.1109/87.294339.

[12] M. Castilla, L. G. de Vicuña, M. López, O. López, and J. Matas, "On the design of sliding mode control schemes for quantum resonant converters," *IEEE Transactions on Power Electronics*, vol. 15, pp. 960–973, Nov. 2000, doi: 10.1109/63.892701.

[13] M. Castilla, L. G. de Vicuña, J. M. Guerrero, J. Matas, and J. Miret, "Sliding-mode control of quantum series-parallel resonant converters via input–output linearization," *IEEE Transactions on Industrial Electronics*, vol. 52, pp. 566–575, Apr. 2005, doi: 10.1109/TIE.2005.844256.

[14] M. Castilla, L. G. de Vicuña, J. Matas, J. Miret, and J. C. Vasquez, "A comparative study of sliding-mode control schemes for quantum series resonant inverters," *IEEE Transactions on*

Industrial Electronics, vol. 56, pp. 3487–3495, Sep. 2009, doi: 10.1109/TIE.2009.2022517.

[15] L. G. de Vicuña, M. Castilla, J. Miret, J. Matas, and J. M. Guerrero, "Sliding-mode control for a single-phase AC/AC quantum resonant converter," *IEEE Transactions on Industrial Electronics*, vol. 56, pp. 3496–3504, Sep. 2009, doi: 10.1109/TIE.2009.2026766.

[16] D. Dong and I. R. Petersen, "Sliding mode control of quantum systems," *New Journal of Physics*, vol. 11, pp. 105033–105050, Oct. 2009, doi: 10.1088/1367-2630/11/10/105033.

[17] D. Dong and I. R. Petersen, "Sliding mode control of two-level quantum systems," *Automatica*, vol. 48, pp. 725–735, Mar. 2012, doi: 10.1016/j.automatica.2012.02.003.

[18] D. Dong and I. R. Petersen, "Sliding mode control of quantum systems," in *Learning and Robust Control in Quantum Technology* (Communications and Control Engineering). Cham: Springer, 2023, doi: 10.1007/978-3-031-20245-2_6.

[19] M. M. Zirkohi, "Fast terminal sliding mode control design for position control of induction motors using adaptive quantum neural networks," *Applied Soft Computing*, vol. 115, pp. 108268–108282, Dec. 2021, doi: 10.1016/j.asoc.2021.108268.

[20] Z. Tavanaei-Sereshki and M. R. Ramezani-al, "Quantum genetic sliding mode controller design for depth control of an underwater vehicle," *Measurement and Control*, vol. 51, pp. 336–348, Jun. 2018, doi: 10.1177/0020294018789199.

[21] J. J. Moghaddam and A. Bagheri, "Suppressing vibration in a multilayers composite material plate using quantum-behaved particle swarm optimization and sliding mode control system," *Proceedings of the Institution of Mechanical Engineers, Part G: Journal of Aerospace Engineering*, vol. 229, pp. 2095–2105, Nov. 2014, doi: 10.1177/0954410014565678.

[22] F. Chen, R. Jiang, C. Wen, and R. Su, "Self-repairing control of a helicopter with input time delay via adaptive global sliding mode control and quantum logic," *Information Sciences*, vol. 316, pp. 123–131, Apr. 2015, doi: 10.1016/j.ins.2015.04.023.

[23] S. Chegini and M. Yarahmadi, "Quantum sliding mode control via error sliding surface," *Journal of Vibration and Control*, vol. 24, pp. 5345–5352, Dec. 2017, doi: 10.1177/1077546317752848.

[24] R. B. Griffiths, *Consistent Quantum Theory*. Cambridge: Cambridge University Press, pp. 95–100, 2002.

[25] D. McMahon, *Quantum Computing Explained*. Hoboken, New Jersey: Wiley, pp. 11–37, 2007.

[26] J. Abhijith, A. Adedoyin, J. Ambrosiano, P. Anisimov, W. Casper, G. Chennupati, C. Coffrin, H. Djidjev, D. Gunter, S. Karra, N. Lemons, S. Lin, A. Malyzhenkov, D. Mascarenas, S. Mniszewski, B. Nadiga, D. O'Malley, D. Oyen, S. Pakin, L. Prasad, R. Roberts, P. Romero, N. Santhi, N. Sinitsyn, P. J. Swart, J. G. Wendelberger, B. Yoon, R. Zamora, W. Zhu, S. Eidenbenz, A. Bärtschi, P. J. Coles, M. Vuffray, and A. Y. Lokhov, "Quantum algorithm implementations for beginners," *ACM Transactions on Quantum Computing*, vol. 24, pp. 1–92, Jul. 2022, doi: 10.1145/3517340.

[27] N. Zioui, A. Mahmoudi, Y. Mahmoudi, and M. Tadjine, "Quantum computing based state domain equations and feedback control," *Results in Applied Mathematics*, vol. 19, pp. 100385–100393, Aug. 2023, doi: 10.1016/j.rinam.2023.100385.

[28] IBM, "IBM quantum composer," 2023. [Online]. Available: https://quantum-computing.ibm.com/composer/files/new